Measurement of radiative neutralino production

Christoph Bartels[1], Olaf Kittel[2]*, Ulrich Langenfeld[3]†, Jenny List[1]

1- DESY, Notkestrasse 85, D-22607 Hamburg, Germany

2- Departamento de Física Teórica y del Cosmos and CAFPE,
Universidad de Granada, E-18071 Granada, Spain

3- Institut für Theoretische Physik und Astronomie,
Universität Würzburg, Am Hubland, D-97074 Würzburg, Germany

We perform the first experimental study with full detector simulation for the radiative production of neutralinos at the linear collider, at $\sqrt{s} = 500$ GeV and realistic beam polarizations. We consider all relevant backgrounds, like the Standard Model background from radiative neutrino production. The longitudinal polarized beams enhance the signal and simultaneously reduce the background, such that statistical errors are significantly reduced. We find that the photon spectrum from the signal process can be well isolated. The neutralino mass and the cross section can be measured at a few per-cent level, with the largest systematic uncertainties from the measurement of the beam polarization and the beam energy spectrum.

1 Introduction

The Minimal Supersymmetric Standard Model (MSSM) is a promising extension of the Standard Model of particle physics (SM) [1]. At a future Linear Collider (LC), the masses, decay widths, couplings, and spins of the new SUSY particles can be measured with high precision [2]. In particular, the lightest electroweak states like pairs of neutralinos, charginos, and sleptons, can be studied in the initial stage of the LC, with a center-of-mass energy $\sqrt{s} = 500$ GeV, and a luminosity of order $\mathcal{L} = 500$ fb^{-1}. The lightest visible SUSY state is a pair of radiatively produced neutralinos [3–6]

$$e^+ + e^- \to \tilde{\chi}_1^0 + \tilde{\chi}_1^0 + \gamma. \tag{1}$$

The signal is a single high energetic photon, radiated off the incoming beams or off the exchanged selectrons, and missing energy from the neutralinos. The main irreducible Standard Model background is photons from radiatively produced neutrinos $e^+e^- \to \nu\bar{\nu}\gamma$, see Fig. 2. Indeed, due to this large background, radiative neutralino production cannot be observed at LEP [5], not even for light or even massless neutralinos [7].

The discovery potential for the radiative production of light neutralinos is much better for the LC, since it provides high luminosity and the option of polarized beams [8]. In particular, it was shown that the electron and positron beam polarizations can be used to significantly enhance the signal and suppress the background from radiative neutrino production simultaneously [3, 5, 6]. This applies in particular for scenarios where the lightest neutralino is mainly bino, i.e., has an enhanced coupling to the right sleptons. Right slepton exchange can be enhanced with positive electron and negative positron beam polarizations.

*Speaker

†U. L. has been supported by funding from the research training group GRK 1147 of the Deutsche Forschungsgemeinschaft and partially by the Helmholtz alliance 'Physics at the Terascale.

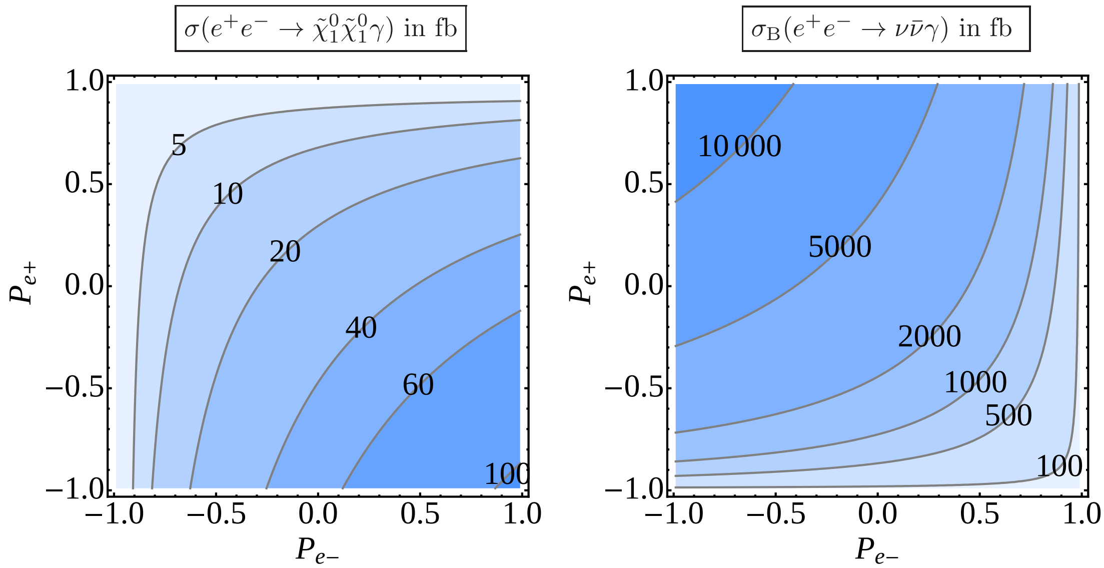

Figure 1: Contour lines of the tree-level cross section [5, 6] for radiative neutralino production, $e^+e^- \to \tilde{\chi}_1^0\tilde{\chi}_1^0\gamma$ (left) and radiative neutrino production $e^+e^- \to \nu\bar{\nu}\gamma$ (right), at the LC for $\sqrt{s} = 500$ GeV and $\mathcal{L} = 500$ fb^{-1}, for our benchmark scenario, Eq. (2). We applied regularization cuts on the photon angle $|\cos\theta_\gamma| \leq 0.99$, and energy $5 \leq E_\gamma[\text{GeV}] \leq 212$.

Since such an adjustment reduces the couplings to the W bosons, radiative neutrino production can be severely suppressed at the same time. In Fig. 1, we show the beam polarization dependence of signal and background, for our benchmark scenario with the relevant low energy SUSY parameters

$$M_1 = 103 \text{ GeV}, \; M_2 = 193 \text{ GeV}, \; \mu = 396 \text{ GeV}, \; \tan\beta = 10, \; m_{\tilde{e}_{R(L)}} = 125(190) \text{ GeV}, \quad (2)$$

where the lightest neutralino $m_{\tilde{\chi}_1^0} = 98$ GeV has a bino component of $N_{11} = 0.986$. Already for a realistic beam polarization of $(P_{e^-}, P_{e^+}) = (0.8, -0.3)$, we obtain large signal to background ratios. The electroweak parameters of our scenario correspond to the widely studied SPS1a′ point [2]. Note that although the first generation squarks and gluinos below about 1 TeV are excluded by recent LHC data [9], if their masses are roughly equal, the QCD sector of the SPS1a′ point is not relevant for our study.

2 Experimental analysis

Due to the large number of signal and irreducible background events in this channel, systematic uncertainties of the detector measurements and of the beam parameters have to be considered. Therefore we perform an experimental study [10–12], to demonstrate the potential of a LC for measuring the production cross section and the $\tilde{\chi}_1^0$ mass. The analysis is made in the framework of the proposed International Linear Collider (ILC) [13] in full simulation of the International Large Detector concept (ILD) [14], and is valid for the nominal ILC parameter set as given in the ILC Reference Design Report (RDR) [13]. The study

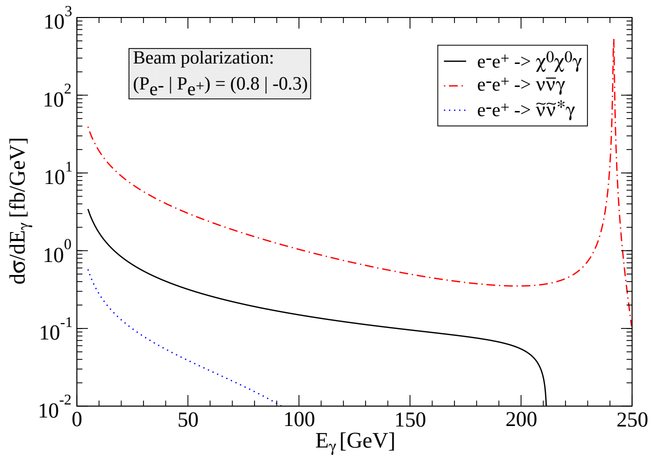

Figure 2: Photon energy distributions for $e^+e^- \to \tilde{\chi}_1^0\tilde{\chi}_1^0\gamma$ (black, solid), $e^+e^- \to \nu\bar{\nu}\gamma$ (red dot-dashed), and $e^+e^- \to \tilde{\nu}\tilde{\nu}^*\gamma$ (blue, dotted), at the LC for $\sqrt{s} = 500$ GeV, $\mathcal{L} = 500$ fb^{-1}, and $(P_{e^-}, P_{e^+}) = (0.8, -0.3)$, for scenario Eq. (2), with regularization cut $|\cos\theta_\gamma| \leq 0.99$ [5].

which we shortly outline here [11], is a model specific application of the model independent study to search for WIMP Dark Matter at the ILC [12, 15], for further details see Ref. [10].

2.1 Background and event generation

Apart from the dominant irreducible SM background process of radiative neutrino pair production $e^+e^- \to \nu\nu\gamma(N)\gamma$ with up to three final state photons $(N = 0, 1, 2)$, additional SM processes have been considered: Radiative Bhabha scattering $e^+e^- \to e^+e^-\gamma$ with forward peaked final state electrons, leaving the detector through the beam pipe or hitting the forward calorimeters, as well as multi-photon final states $e^+e^- \to \gamma\gamma(N)\gamma$, where only one of the emitted photons is properly reconstructed.

For the event generation, Whizard [16, 17] has been initialized with the ILC baseline parameter set for a $\sqrt{s} = 500$ GeV machine [13]. The production of initial state radiation (ISR) in the leading logarithm approximation [16] is switched on, resulting in up to two predominantly soft and collinear additional photons. The beam energy spectrum used in the event generation has been calculated using GuineaPig [18].

2.2 Detector simulation

For the detector simulation the Geant4 [19] based Mokka [20] simulation software has been used. The event reconstruction was performed with the PandoraPFA [21] reconstruction algorithm used within the MarlinReco [22] reconstruction framework for linear colliders. After simulation, two corrections are performed on the reconstructed event samples. In a first step, split uncharged electromagnetic clusters are iteratively merged with a cone based method to form higher level photon candidates. A second correction re-calibrates the detected photon energies with respect to energy lost in the cracks and inter-module gaps for cabling and readout of the ILD [10].

	$(\lvert P_{e^-}\rvert;\ \lvert P_{e^+}\rvert)\ =\ (0.8;\,0.3)$	$(\lvert P_{e^-}\rvert;\ \lvert P_{e^+}\rvert)\ =\ (0.8;\,0.6)$
σ_{RL}/σ_0	3.89 ± 0.8 (0.5)	3.89 ± 0.3 (0.2)
σ_{RR}/σ_0	0.00 ± 1.1 (0.7)	0.00 ± 0.8 (0.5)
σ_{LL}/σ_0	0.00 ± 1.2 (1.0)	0.00 ± 0.8 (0.5)
σ_{LR}/σ_0	0.11 ± 1.3 (0.8)	0.11 ± 1.0 (0.5)

Table 1: Measured fully polarized cross sections $\sigma_{\{R,L\}}/\sigma_0 \pm \delta_\sigma$ [fb], see Eq. (5), for two different positron polarizations for scenario Eq. (2). The error δ_σ is the squared sum of the statistical and the systematic errors. The values in brackets correspond to an improved polarization measurement of $\delta P = 0.1\%$, instead of $\delta P = 0.25\%$.

2.3 Event sampling and selection cuts

In order to enable an efficient study of many different models, the signal events were generated by reweighting the fully simulated SM background samples. To avoid statistical correlation, the background samples have been divided into three statistically independent subsamples. The first two subsamples are used for the background and signal contribution to the data. The third sample is parametrized to yield the predicted photon spectra.

Since the $\nu\nu\gamma$ SM background is indistinguishable on an event-by-event basis from the neutralino signal, the selection is tuned to isolate this SM background. An event is considered signal-like when it contains at least one photon with

$$10\ \text{GeV} < E_\gamma < 220\ \text{GeV}, \qquad |\cos\theta_\gamma| < 0.98. \tag{3}$$

This signal definition ensures that the detected photons are within the tracking acceptance of the ILD detector to distinguish them from charged particles. The cut on the photon energy reduces the contributions from soft ISR, and excludes the massless neutrino final states from the radiative Z-return at photon energies of 241 GeV, see Fig. 2.

In the further event selection, the following constraints are set to reject the dominant reducible SM backgrounds. To exclude hadronic and leptonic final states, a cut $E_{\text{vis}} - E_\gamma < 20$ GeV is applied on the maximal exclusive energy, i.e., the total detected (visible) event energy excluding the selected photon. The maximal transverse track momentum is constrained to $p_T < 3$ GeV. Low p_T tracks have to be allowed because of track overlays from e^+e^- pairs from the beamstrahlung background, and from multi-peripheral $\gamma\gamma \to$ hadrons events. Although the angular distribution of the final state fermions is strongly peaked in the forward direction, a strong activity in the sensitive volume is expected, due to the large cross section in the order of 5×10^8 fb. The impact of both contributions has been studied for the ILD detector using Whizard for event generation [14]. The beamstrahlung spectrum has been simulated with Guinea Pig. On average 0.7 tracks from $\gamma\gamma$ processes and 1.5 tracks from beamstrahlung background are expected per bunch crossing. Tight selection criteria on these tracks would therefore reduce the signal statistic strongly. Finally, the large Bhabha background is reduced by an identification of high energy electrons in the forward beam calorimetry. The selection efficiency of the $\nu\nu\gamma$ background is above 80% on average, while the multi-photon and Bhabha background is reduced to < 1%. The signal selection efficiency is about 92%.

2.4 Cross section measurement and coupling structure

The signal cross section is determined by a subtraction of the expected number of background events $< N_B >$ from the number of observed data events N_D,

$$\sigma(P_{e^-}, P_{e^+}) \quad = \quad \frac{N_D - < N_B >}{\mathcal{L} \times \varepsilon}, \tag{4}$$

with the experimental luminosity $\mathcal{L}$ and the signal efficiency ε. With four different polarization configurations, the fully polarized cross sections $\sigma_{\{L,R\}}$, and hence the helicity structure of the coupling to the beam electrons, can be determined from [8]

$$\begin{aligned} \sigma(P_{e^-}, P_{e^+}) \quad = \quad & \frac{1}{4}\Big[(1 + P_{e^-})(1 + P_{e^+})\sigma_{RR} + (1 - P_{e^-})(1 - P_{e^+})\sigma_{LL} \\ & + \ (1 + P_{e^-})(1 - P_{e^+})\sigma_{RL} + (1 - P_{e^-})(1 + P_{e^+})\sigma_{LR}\Big]. \end{aligned} \tag{5}$$

In Tab. 1, we summarize the reconstructed cross sections and their corresponding errors. The luminosity of $\mathcal{L} = 500\ \text{fb}^{-1}$ is distributed to the odd (even) sign polarization configurations with $\mathcal{L} = 200\,(50)\ \text{fb}^{-1}$ each. With an assumed systematic polarization measurement error of $\delta P = 0.25\%$ [23], the cross section σ_{RL} can be determined to a level of about 20 (7)%, for an positron polarization of $|P_{e^+}| = 0.3\,(0.6)$. Since the systematic uncertainty is dominated by the precision of the polarization measurement δP, the systematic error can be reduced by about a third if $\delta P = 0.1\%$ could be achieved, see Tab. 1. At the ILC, the long term average of the luminosity weighted beam polarization can be determined from collision data to 0.17% for both electrons and positrons with $|P_{e^+}| = 0.6$, dominated by the uncertainties from the polarimeters [24]. Under the assumption of uncorrelated polarization errors, a combination of the measured fully polarised cross sections $\sigma_{\{L,R\}}$ yields an uncertainty of 9.3 (6.0)% on the cross section for unpolarised beams for $\delta P = 0.25\%$ and $|P_{e^+}| = 0.3\,(0.6)$, again systematically dominated by the polarimeters.

2.5 Neutralino mass measurement

The mass of the neutralino candidate is determined from a χ^2 fit of the full data energy spectrum to template spectra with different masses. Depending on the degree of positron polarization, statistical precisions of 1.7 to 2.6 GeV can be obtained for an integrated luminosity of 500 fb^{-1}. The total uncertainty on the candidate mass is dominated by the uncertainty in the beam energy spectrum, contributing with an error of 2.2 GeV to the mass determination, see Tab. 2. The influence of the beam energy spectrum, which distorts the energy spectrum of the signal photon, has been estimated by generation of signal spectra in a generic WIMP model [15] for two different sets of beam parameters, RDR [13] and SB-2009 [25]. This is a conservative estimate, since the beam energy spectrum will be known to a higher degree than the difference between the sets.

$m_{\tilde{\chi}_1^0}$ [GeV]	$\pm$ stat. $\pm$ sys. ($\delta E \pm \delta\mathcal{L}$) (total) [GeV]	(P_{e^-}; P_{e^+})
97.7	$\pm$ 2.65 $\pm$ 0.09 $\pm$ 2.20 (3.44)	(0.8; 0.0)
97.7	$\pm$ 2.07 $\pm$ 0.09 $\pm$ 2.20 (3.02)	(0.8; −0.3)
97.7	$\pm$ 1.70 $\pm$ 0.09 $\pm$ 2.20 (2.79)	(0.8; −0.6)

Table 2: Neutralino mass determined from a template comparison for an integrated luminosity of $\mathcal{L} = 500$ fb^{-1} and different beam polarizations. The systematic uncertainties comprise of the beam energy scale calibration (δE) and the beam energy spectrum ($\delta\mathcal{L}$).

References

[1] H. E. Haber and G. L. Kane, Phys. Rept. **117**, 75 (1985).

[2] J. A. Aguilar-Saavedra *et al.*, Eur. Phys. J. C **46**, 43 (2006) [arXiv:hep-ph/0511344].

[3] S. Y. Choi, J. S. Shim, H. S. Song, J. Song and C. Yu, Phys. Rev. D **60** (1999) 013007 [arXiv:hep-ph/9901368].

[4] H. Baer and A. Belyaev, arXiv:hep-ph/0111017.

[5] H. K. Dreiner, O. Kittel and U. Langenfeld, Phys. Rev. D **74** (2006) 115010 [arXiv:hep-ph/0610020].

[6] H. K. Dreiner, O. Kittel and U. Langenfeld, Eur. Phys. J. C **54**, 277 (2008) [arXiv:hep-ph/0703009].

[7] H. K. Dreiner, S. Heinemeyer, O. Kittel, U. Langenfeld, A. M. Weber, G. Weiglein, Eur. Phys. J. **C62**, 547-572 (2009). [arXiv:0901.3485 [hep-ph]].

[8] G. Moortgat-Pick *et al.*, Phys. Rept. **460**, 131 (2008) [arXiv:hep-ph/0507011].

[9] G. Aad *et al.* [ATLAS Collaboration], Phys. Rev. D **85**, 012006 (2012) [arXiv:1109.6606 [hep-ex]]; S. Chatrchyan *et al.* [CMS Collaboration], Phys. Rev. Lett. **107**, 221804 (2011) [arXiv:1109.2352 [hep-ex]].

[10] C. Bartels, Diploma Thesis, *Model-independent WIMP searches at the ILC*, DESY 2007; C. Bartels, PhD Thesis, *WIMP search and a Cherenkov detector prototype for ILC polarimetry*, DESY-THESIS-2011-034.

[11] `http://ilcagenda.linearcollider.org/contributionDisplay.py?contribId=263&sessionId=6&confId=5134`

[12] `http://ilcagenda.linearcollider.org/contributionDisplay.py?contribId=257&sessionId=6&confId=5134`

[13] N. Phinney, ICFA Beam Dyn. Newslett. **42** (2007) 7.

[14] T. Abe *et al.* [ILD Concept Group - Linear Collider Collaboration], arXiv:1006.3396 [hep-ex].

[15] A. Birkedal, K. Matchev and M. Perelstein, Phys. Rev. D **70** (2004) 077701 [arXiv:hep-ph/0403004].

[16] W. Kilian, T. Ohl and J. Reuter, Eur. Phys. J. C **71** (2011) 1742 [arXiv:0708.4233 [hep-ph]].

[17] M. Moretti, T. Ohl and J. Reuter, arXiv:hep-ph/0102195.

[18] D. Schulte, TESLA 97-08 (1996).

[19] S. Agostinelli *et al.* [GEANT4 Collaboration], Nucl. Instrum. Meth. A **506**, 250 (2003).

[20] Mokka, `http://polzope.in2p3.fr:8081/MOKKA`

[21] M. A. Thomson, Nucl. Instrum. Meth. A **611** (2009) 25 [arXiv:0907.3577 [physics.ins-det]].

[22] MarlinReco, `http://ilcsoft.desy.de/portal/software\_packages/marlinreco`

[23] S. Boogert *et al.*, JINST **4** (2009) P10015 [arXiv:0904.0122 [physics.ins-det]].

[24] I. Marchesini, DESY-THESIS-2011-044.

[25] M. Berggren, arXiv:1007.3019 [hep-ex].